Neuron
Article

Loss of Sensory Input Causes Rapid Structural Changes of Inhibitory Neurons in Adult Mouse Visual Cortex

Tara Keck,[1,3] Volker Scheuss,[1] R. Irene Jacobsen,[1,3] Corette J. Wierenga,[1] Ulf T. Eysel,[2] Tobias Bonhoeffer,[1] and Mark Hübener[1,*]
[1]Max Planck Institute of Neurobiology, Am Klopferspitz 18, D-82152 Martinsried, Germany
[2]Department of Experimental Neurophysiology, Ruhr University Bochum, Universitätsstrasse 150, D-44780 Bochum, Germany
[3]Present address: MRC Centre for Developmental Neurobiology, King's College London, Guy's Campus, New Hunt's House, London, SE1 1UL, UK
*Correspondence: mark@neuro.mpg.de
DOI 10.1016/j.neuron.2011.06.034

SUMMARY

A fundamental property of neuronal circuits is the ability to adapt to altered sensory inputs. It is well established that the functional synaptic changes underlying this adaptation are reflected by structural modifications in excitatory neurons. In contrast, the degree to which structural plasticity in inhibitory neurons accompanies functional changes is less clear. Here, we use two-photon imaging to monitor the fine structure of inhibitory neurons in mouse visual cortex after deprivation induced by retinal lesions. We find that a subset of inhibitory neurons carry dendritic spines, which form glutamatergic synapses. Removal of visual input correlates with a rapid and lasting reduction in the number of inhibitory cell spines. Similar to the effects seen for dendritic spines, the number of inhibitory neuron boutons dropped sharply after retinal lesions. Together, these data suggest that structural changes in inhibitory neurons may precede structural changes in excitatory circuitry, which ultimately result in functional adaptation following sensory deprivation.

INTRODUCTION

Cortical circuits are dynamic and they adapt to novel inputs and altered sensory environments, even through adulthood. Recent in vivo two-photon imaging studies have investigated the degree to which functional plasticity induced by sensory deprivation (Hofer et al., 2009; Holtmaat et al., 2006; Keck et al., 2008; Majewska et al., 2006; Trachtenberg et al., 2002; Yamahachi et al., 2009; Yang et al., 2009; Zuo et al., 2005) or motor learning (Komiyama et al., 2010; Xu et al., 2009) correlates with structural plasticity, specifically of dendritic spines—the postsynaptic, structural specializations on many neuronal cell types, most notably pyramidal cells. Spines on excitatory cells carry synapses in the vast majority of cases (Arellano et al., 2007; Harris and Stevens, 1989; Knott et al., 2006; Nägerl et al., 2007) and therefore serve as convenient structural correlates of synapses, which has eased the study of synaptic changes in vivo and allowed for following the fate of individual synapses over extended periods of time (Grutzendler et al., 2002; Hofer et al., 2009; Holtmaat et al., 2006; Keck et al., 2008; Majewska et al., 2006; Trachtenberg et al., 2002; Xu et al., 2009; Yang et al., 2009; Zuo et al., 2005). Dendritic spines are conventionally believed to be largely absent from inhibitory neurons; however, there have been occasional reports of their presence on inhibitory neurons in cortex (Azouz et al., 1997; Kawaguchi et al., 2006; Kuhlman and Huang, 2008; Peters and Regidor, 1981), and in hippocampus (Freund and Buzsáki, 1996; Martínez et al., 1999). Owing to the fact that only few inhibitory neurons carry spines, studies of structural plasticity in cortical inhibitory neurons thus far have primarily focused on changes to the branch tips of dendrites (Chen et al., 2011; Lee et al., 2006, 2008). The potential plasticity of dendritic spines on cortical inhibitory neurons in both the naive brain and following sensory deprivation is still unexplored.

Similarly, axonal boutons can serve as a structural marker for presynaptic components in chronic in vivo imaging experiments (De Paola et al., 2006; Stettler et al., 2006). These studies have shown that axonal boutons of excitatory cells display a baseline turnover in the unperturbed cortex (De Paola et al., 2006; Stettler et al., 2006) and that, like spines, bouton dynamics increase following sensory deprivation in both excitatory (Yamahachi et al., 2009) and inhibitory (Chen et al., 2011; Marik et al., 2010) neurons.

While the importance of inhibitory circuits in cortical plasticity is well established in juvenile animals during the critical period (Hensch, 2005), the role of inhibition is less understood in adult animals. In both functional (Froemke et al., 2007) and anatomical (Chen et al., 2011; Hendry and Jones, 1988; Rosier et al., 1995) studies in adult animals, changes in inhibition seem to occur prior to changes in excitatory connections, over time courses ranging from seconds (Froemke et al., 2007) to days (Chen et al., 2011; Rosier et al., 1995) to months (Hendry and Jones, 1988), suggesting a possible role of reduced inhibition in enhancing plasticity of excitatory connections.

In previous work, we have introduced a retinal lesion paradigm in mice (Keck et al., 2008), which leads to functional alterations

in the visual cortex. Permanent ablation of a small part of the retina leaves a region of the monocular visual cortex temporarily unresponsive. As had been described previously (Calford et al., 2003; Giannikopoulos and Eysel, 2006; Gilbert and Wiesel, 1992; Heinen and Skavenski, 1991; Kaas et al., 1990), in the weeks and months following the retinal lesion, the cortical "lesion projection zone" (LPZ) reorganizes functionally and regains responsiveness to visual stimuli. The functional reorganization is believed to occur largely within the cortex (Gilbert and Wiesel, 1992), as there is only very restricted recovery in the lateral geniculate nucleus (LGN, Eysel, 1982). Reorganization is accompanied by cortical structural plasticity, such as increased spine dynamics in layer 5 pyramidal neurons in the LPZ (Keck et al., 2008) and axonal sprouting of layer 2/3 pyramidal cells into the LPZ from adjacent regions of cortex (Darian-Smith and Gilbert, 1994; Yamahachi et al., 2009).

Here, we use chronic two-photon imaging to examine the structural plasticity of inhibitory neurons following retinal lesions. We make use of transgenic mice expressing GFP under the glutamic acid decarboxylase 65 (GAD65) promoter (López-Bendito et al., 2004). Importantly, a subset of these cells have dendritic spines with excitatory synapses, allowing us to follow synapses on inhibitory cells which, without these spines, are hard to study on the typically smooth dendrites of inhibitory cells. Similar to their counterparts on excitatory cells (Hofer et al., 2009; Holtmaat et al., 2006; Keck et al., 2008; Majewska et al., 2006; Trachtenberg et al., 2002; Zuo et al., 2005), we found these inhibitory neuron spines to display baseline turnover. Shortly after a retinal lesion, the density of inhibitory neuron spines is rapidly and lastingly decreased in the LPZ. Likewise, after a retinal lesion, axonal boutons of inhibitory neurons are rapidly lost, with a slower time course than that observed for spines. These data suggest that following sensory deprivation, there is a drop in the excitatory input to inhibitory neurons, in conjunction with a decrease in the cells' synaptic output. Together, these changes likely act in concert to lower the overall inhibitory drive in the cortex after a loss of sensory input, potentially triggering functional reorganization.

RESULTS

Spines on Inhibitory Neurons

We studied structural plasticity of inhibitory neurons during cortical reorganization using the GAD65-GFP mouse line (López-Bendito et al., 2004). We investigated changes to both the inputs and outputs of these neurons, in order to learn how their synapses change in the unperturbed brain and following sensory deprivation.

A subset of inhibitory neurons in this mouse line (22% of GFP-labeled cells in layers 1 and 2/3 of visual cortex) has dendrites that carry spines (Figure 1A), as had been previously described for some types of cortical inhibitory neurons (Azouz et al., 1997; Kawaguchi et al., 2006; Kuhlman and Huang, 2008; Peters and Regidor, 1981). We carried out immunostainings to confirm that these cells were, in fact, inhibitory neurons and found that all of these spiny cells were positive for GABA and GAD 67 (Figure 1B). Further immunostaining to determine which additional markers were expressed by these spiny inhibitory neurons revealed that a large fraction were neuropeptide Y (NPY) positive (91%; Figures 1B and 1C compared with 21% of all GFP-positive inhibitory neurons that are positive for NPY). Additionally, a smaller fraction of spiny inhibitory cells were calretinin (CR) positive (20%; Figure 1B), while there were hardly any somatostatin (SOM)-positive spiny interneurons (5%). Immunostaining confirmed (López-Bendito et al., 2004) that there were no parvalbumin (PV) positive cells (0/165 GFP cells) labeled in the visual cortex of this mouse line.

While it is well established that nearly all dendritic spines of excitatory neurons receive synaptic inputs (Arellano et al., 2007; Knott et al., 2006; Nägerl et al., 2007), this correlation may not hold for spines of inhibitory neurons. We therefore sought to determine if the inhibitory neuron spines found in this mouse line carried synapses. We performed immunostaining against the vesicular glutamate transporter (VGlut1), a presynaptic marker for glutamatergic synapses, and, in a separate set of animals, against VGAT and gephyrin, pre- and postsynaptic markers for GABAergic synapses. We found that spines were juxtaposed to VGlut1 positive structures at a level much higher than chance (Figures 1D and 1E), but not to VGAT- and gephyrin-positive structures (Figure 1E). In fact, spines colocalized with inhibitory synaptic markers (either one or both markers) at levels significantly lower than chance. Together, these data suggest that the majority of spines on the dendrites of inhibitory neurons carry synapses, and that most of these are from excitatory, but not inhibitory, presynaptic neurons.

Having shown that spines of inhibitory neurons colocalize with markers for excitatory synapses, we next explored if these synapses carried functional receptors. In acute slices of visual cortex, we used whole cell voltage clamp recordings of GFP-expressing spiny inhibitory neurons to measure excitatory postsynaptic currents (EPSCs) evoked by focal two-photon glutamate uncaging. Glutamate uncaging immediately adjacent to spines consistently elicited EPSCs in all spines tested (n = 15, Figures 1F and 1G). Uncaging performed at the same distance from the dendritic shaft in the absence of a spine consistently evoked far smaller responses (Figures 1F and 1G), suggesting that currents were likely elicited through synapses on spines and not the result of glutamate diffusion to synapses located elsewhere. Together, these data show that dendritic spines of inhibitory neurons carry functional glutamatergic receptors.

Dynamics of Spines on Inhibitory Cells

For excitatory pathways, it has been shown that dendritic spines on cortical pyramidal neurons are not stable over time. Even under baseline conditions, new spines grow and existing ones disappear (Grutzendler et al., 2002; Hofer et al., 2009; Holtmaat et al., 2006; Keck et al., 2008; Majewska et al., 2006; Trachtenberg et al., 2002; Zuo et al., 2005). To examine whether interneuron spines show a similar behavior, we used repeated two-photon imaging in the monocular visual cortex of adult (p80-100) GAD65-GFP mice (López-Bendito et al., 2004; Wierenga et al., 2010). We imaged the dendrites of inhibitory neurons located in layers 1 and 2/3 (0–200 μm below the pial surface). Previous work has reported modifications of dendritic branch tips of inhibitory neurons in visual cortex (Lee et al., 2006, 2008), which increase after plasticity (Chen et al., 2011); however, for

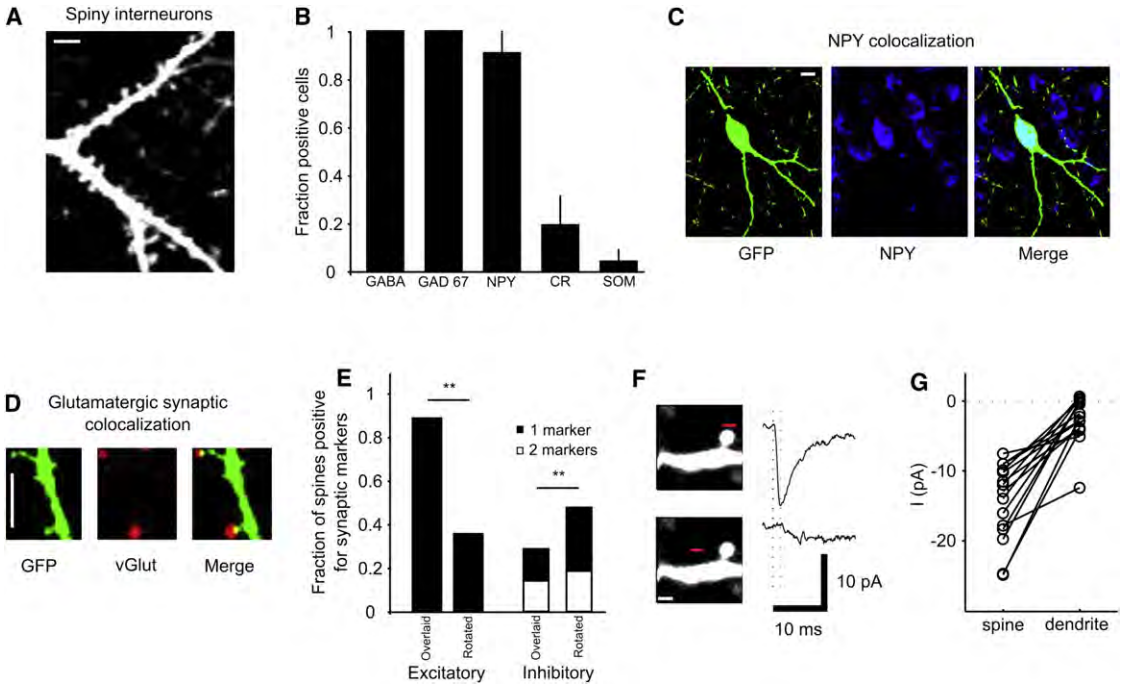

Figure 1. Dendritic Spines on Inhibitory Neurons

(A) Raw single optical section of dendrites of a spiny inhibitory neuron. Scale bar, 5 μm.

(B) Fraction of spiny inhibitory neurons (n = 752 cells, 10 mice) positive for a given marker: GABA, GAD 67, Neuropeptide Y (NPY), Calretinin (CR), somatostatin (SOM). Fractions of positive cells were calculated per section.

(C) Example images of a NPY positive cell, showing the GFP-labeled cell (left), anti-NPY immunostaining (center) and the merged image (right). Light blue indicates overlapping pixels. Scale bar, 5 μm.

(D) Immunostaining for vGlut1, a marker for excitatory synapses (middle), GFP labeled dendrite (left), and merged image (right). Yellow indicates overlapping pixels. Scale bar, 5 μm.

(E) Fraction of spines on inhibitory neurons that colocalize with one or both of the inhibitory synapse markers (VGAT and gephyrin) or the excitatory synapse marker VGlut1. "Rotated" indicates that the GFP image was rotated by 90° (comparing overlaid to rotated images, inhibitory synapses, $p < 0.001$; excitatory synapses, $p < 0.01$, n = 30 cells, four mice).

(F) Inhibitory neuron spine and positions of glutamate uncaging (left, red line), and corresponding example traces of uncaging evoked currents recorded with a somatic patch pipette (right). Top, uncaging near spine head; bottom, uncaging next to the dendrite at a distance similar to the spine length. In the right panels, the left dashed line indicates the time of uncaging; the right dashed line indicates the peak of the response from the spine. Scale bar, 1 μm.

(G) Summary of average current amplitudes evoked by uncaging close to spine heads (spine) and dendrites at spine distance (dendrite; n = 15 spines, four cells). All error bars, standard error of the mean (SEM).

the types of interneurons labeled in the GAD65-GFP mouse line used here, we found that dendrites were largely stable. In contrast, and similar to excitatory neurons (Grutzendler et al., 2002; Hofer et al., 2009; Holtmaat et al., 2006; Keck et al., 2008; Majewska et al., 2006; Trachtenberg et al., 2002; Zuo et al., 2005), inhibitory neurons in control animals displayed a stable spine density over time (Figures 2B and 2C, red curve), but lost (and gained) a fraction of spines over a few days (Figure 2D, red curve).

We next tested whether changes in sensory input alter inhibitory neuron spine numbers and dynamics. Indeed, in the 72 hr after inducing focal retinal lesions (Figure 2A), spine turnover increased in the center of the LPZ, such that there was a decrease in the density (Figures 2B and 2C, blue curve) and survival fraction (Figure 2D, blue curve) of spines on inhibitory cells. After this rapid spine loss, we detected no recovery of spine density 1 month (density normalized to value at 72 hr after lesion: 104 ± 7%) or 2 months (normalized density: 98% ± 7%) after the retinal lesion. Careful examination of the dendrites following retinal lesions suggest that structural changes are limited to the spines and that dendritic structures remain stable over time. These data demonstrate a long-lasting loss of excitatory spines on inhibitory neurons in the LPZ following a focal retinal lesion.

In order to determine if the drop in spine density is specific for inhibitory neurons or generalizes to all dendritic spines, we chronically imaged spine density in another set of animals, expressing GFP in mostly excitatory neurons (under the *thy-1* promoter, M-line, Feng et al., 2000). We found no change in the spine density of excitatory neurons measured 72 hr after a retinal lesion (Figure 2E), suggesting that our results are specific to inhibitory neurons.

We have previously reported that structural changes to spines on excitatory cells following retinal lesions were localized to the LPZ (Keck et al., 2008). We therefore examined the spatial extent of the inhibitory neuron spine loss in the visual cortex. Even

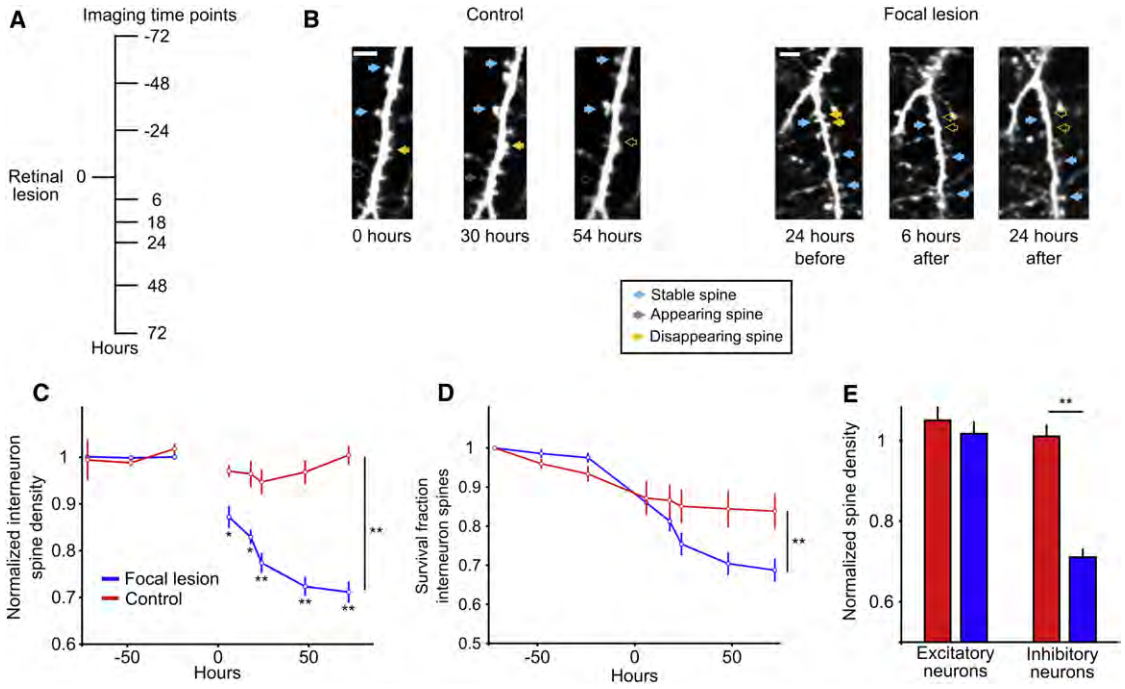

Figure 2. Structural Dynamics of Spines on Inhibitory Neuron Dendrites

(A) Time line of experimental protocol. Two-photon imaging was carried out at each time point, except at 0 hr, at which time the retinal lesion was induced.

(B) z-projected images of spines on inhibitory neurons in control (left) and lesioned (right) animals. Arrows show disappearing (yellow), appearing (gray) and stable (blue) spines. Filled arrows indicate that the spine is present, hollow arrows indicate that the spine is absent. Scale bar, 5 μm.

(C) Normalized (average of first three time points) spine density in the center of the LPZ decreases in focally lesioned animals (blue) within 6 hr of a lesion ($p < 0.05$). Density in control animals (red) does not change.

(D) Survival fraction of spines. More spines are lost in lesioned than in control animals ($p < 0.01$).

(E) Following a retinal lesion (72 hr), spine density of excitatory neurons stays constant, but drops on inhibitory neurons ($p < 0.01$). For each cell, density is normalized to the average of the first three time points.

(C and D: n = 15 cells, eight animals; E: n = 43 cells, 20 animals).

All error bars, SEM.

inhibitory neurons whose cell body and dendrites were located outside the LPZ (as determined by intrinsic signal imaging 72 hr after the retinal lesion) showed a substantial decrease in spine density (Figure 3A). Spine density measured 72 hr after lesion was correlated with the distance of the cell body from the border of the LPZ ($R = 0.48$; $p = 0.02$), such that cells located near to the LPZ had densities similar to cells in the LPZ and cells further away from the LPZ had densities similar to control animals (Figure 3B). Thus, inhibitory neurons outside the directly silenced cortical region are also affected—albeit to a lesser degree—by the altered sensory input.

The observed lasting loss of spines following retinal lesions could have two possible explanations. One possibility is that these changes reflect competition between lost and preserved visual inputs in the LPZ during functional reorganization of the retinotopic map (Keck et al., 2008). Alternatively, because activity levels in the LPZ are reduced following retinal lesions, changes to the spines could simply reflect the overall reduction in cortical activity. For spines on excitatory neurons, we have previously described that structural dynamics increased following complete input removal, but to a much lesser extent than during functional reorganization after focal retinal lesions (Keck et al., 2008). These results suggest that increased excitatory spine dynamics following sensory deprivation are not simply caused by reduced cortical activity levels, but rather depend on competition between deprived and non-deprived inputs.

To distinguish between these two alternative explanations for spine changes in inhibitory neurons, we performed complete bilateral retinal lesions, removing all visually evoked input, thus preventing the functional reorganization that is observed following focal retinal lesions. As expected, these mice were unresponsive to visual stimuli and demonstrated no functional recovery over the months following the complete retinal lesion (Keck et al., 2008). The density (Figures 3C and 3D) as well as the survival fraction (Figure 3E) of spines on inhibitory neurons decreased in the 48 hr following complete retinal lesions to the same degree as we had found after focal lesions. Inhibitory neuron spine density decreased significantly 6 hr after focal lesions but only 48 hr following complete lesions, indicating that the exact timing of structural changes depends on the nature of the deprivation (see Discussion).

Inhibitory Neuron Bouton Dynamics

So far, we have shown that inhibitory neurons lose a substantial fraction of their excitatory inputs, suggesting a lower level of inhibition in the visual cortex after sensory deprivation. Is this

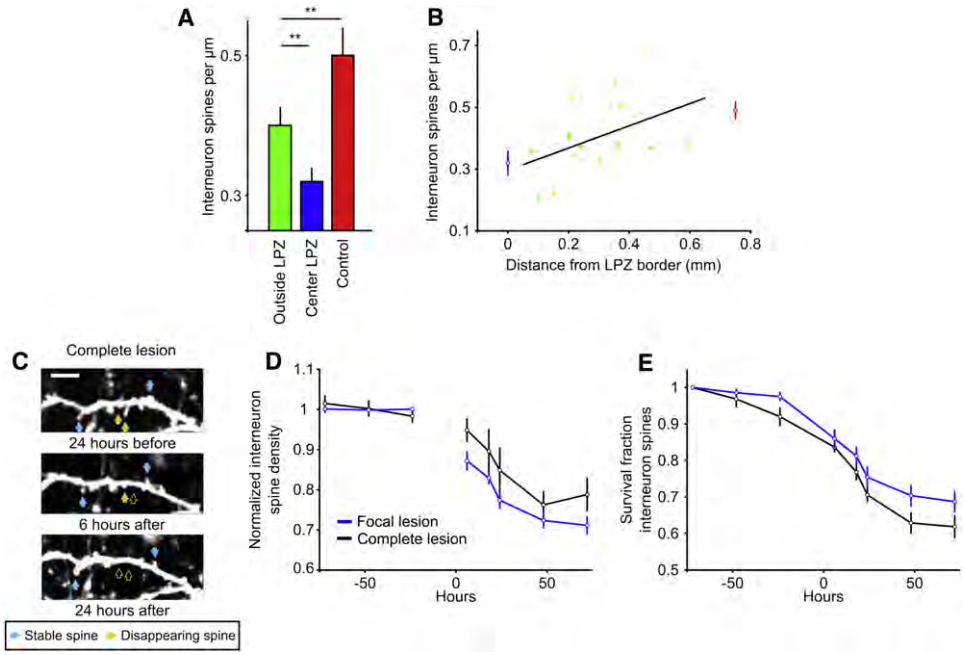

Figure 3. Inhibitory Neuron Spine Loss Is Not Restricted to the LPZ and Follows Decreased Cortical Activity

(A) Outside the LPZ, spine density decreases relative to controls ($p < 0.01$), but to a smaller degree than in the center of the LPZ ($p < 0.01$; $n = 23$ cells, 12 animals). (B) Spine density for individual cells outside the LPZ (green) correlates ($R = 0.48$; $p = 0.02$) with the distance of the soma from the border of the LPZ (at 0 mm). Green circles are individual cells. Red, average density in control animals; blue, average density for cells in the center of the LPZ.

(C–E) (C) z-projected images of spines on inhibitory neurons before and after complete lesions. Arrows show disappearing (yellow) and stable (blue) spines. Filled arrows indicate that the spine is present, hollow arrows indicate that the spine is absent. Scale bar, 5 µm. (D) Normalized spine density in mice with complete lesions decreases (48 hr $p < 0.05$; 72 hr $p < 0.01$) to the same degree as in animals with focal lesions ($p > 0.5$). (E) Survival fraction of spines decreases over time (complete lesion versus control $p < 0.01$). No differences were seen between mice with focal and complete retinal lesions ($p > 0.65$; C and D: $n = 12$ cells, 8 animals).

All error bars, SEM.

also reflected on the output side (i.e., axons and boutons) of these cells? In control animals, chronic two-photon imaging did not reveal any changes in the overall axonal architecture over a period of 6 days, but we observed a baseline turnover of axonal boutons. Similar to boutons on excitatory axons (De Paola et al., 2006; Stettler et al., 2006), the overall density of boutons on inhibitory axons remains constant over time (Figures 4A and 4C, red curve), but boutons are constantly added and lost over time (Figure 4D, red curve).

To determine if baseline structural dynamics are altered by sensory deprivation, we measured changes in inhibitory axons and boutons in the 72 hr before and after a focal retinal lesion (Figure 4B). Using intrinsic signal imaging, we localized the LPZ (Keck et al., 2008) and performed two-photon imaging of inhibitory neurons in layers 1 and 2/3 located in the center of the deprived cortical region. Examination of axonal branches did not reveal any change to the axonal architecture in lesioned animals. In contrast, we found clear and rapid changes of inhibitory boutons. Similar to dendritic spines of inhibitory neurons, inhibitory cell bouton density dropped massively within 24 hr of the lesion (Figures 4B and 4C; 24 hr: 0.44 ± 0.02 boutons/µm axon; corresponding to 84% ± 2% of the original value measured before lesions). After these initial changes, bouton density remained relatively constant, such that 1–2 months later the density is the same as measured 24 hr after the lesion (1 month: 0.44 ± 0.03 boutons/µm axon; 2 months: 0.45 ± 0.03 boutons/µm axon). In line with the drop in density, fewer of the boutons that were initially present survive following a retinal lesion (Figure 4D).

To exclude that the bouton loss was a consequence of the imaging per se, we measured bouton density in a separate group of mice 72 hr after a retinal lesion, without any prior imaging. In these animals, inhibitory bouton density was also decreased (Figure 4E, 0.44 ± 0.03 boutons/µm axon), to levels similar to those observed with more frequent imaging (72 hr; 0.45 ± 0.02 boutons/µm axon). Thus, repeated imaging does not induce bouton loss. Furthermore, the decreased bouton density was specific for inhibitory cells, as bouton density on excitatory cells (measured in separate experiments using a mouse line expressing GFP in mostly excitatory neurons under the *thy-1* promoter, M line, Feng et al., 2000) did not decrease 72 hr after a retinal lesion (Figure 4F).

To determine the spatial extent of these changes in bouton density, we measured the structural dynamics of cells whose axons were located outside the LPZ. Similar to what we found for the spines on inhibitory cells (Figure 3A), there was a decrease in bouton density even outside of the LPZ (Figure 5A). There was a clear correlation between bouton density and distance of

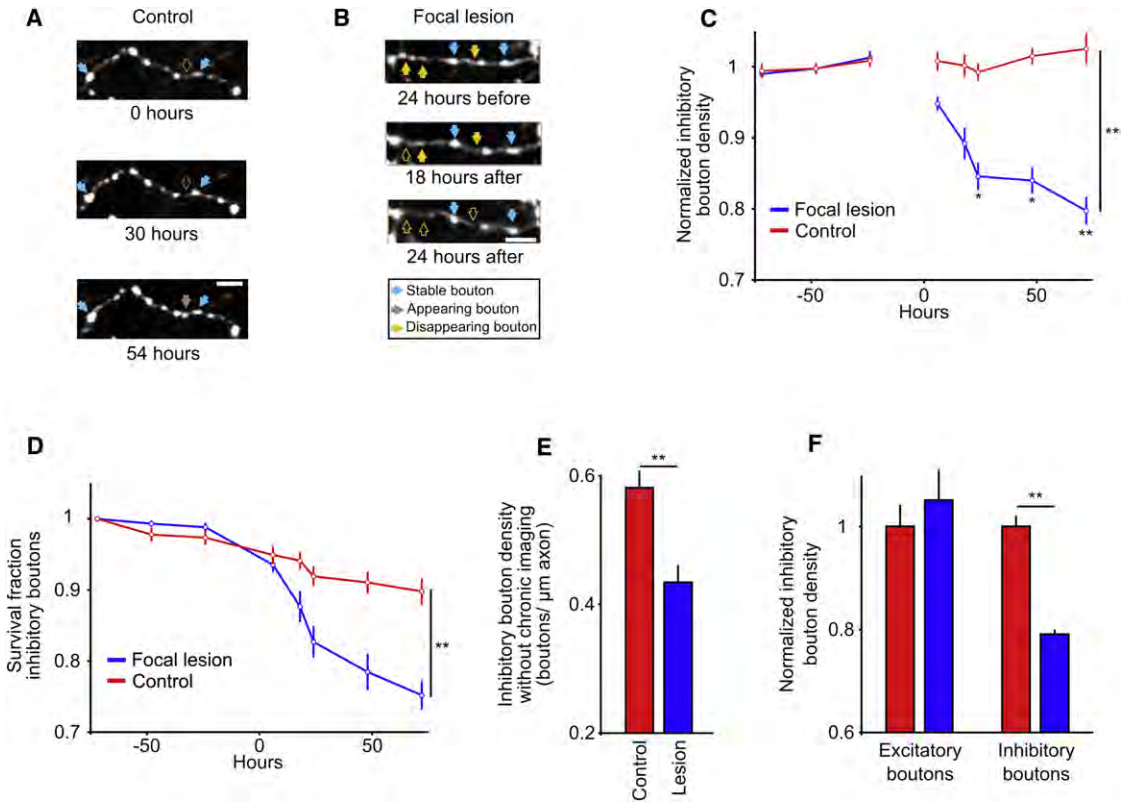

Figure 4. Rapid Drop in GABAergic Bouton Density in the Visual Cortex following Retinal Lesions

(A and B) Example of z-projected images of the same stretch of axon over time in a control (A) and focally lesioned (B) animal. Arrows show appearing (gray), disappearing (yellow) and stable (blue) boutons. Filled arrows indicate that the bouton is present, hollow arrows indicate that the bouton is absent. Scale bar, 5 µm.

(C) For (C)–(F), data from focally lesioned and control mice are shown in blue and red, respectively. Bouton density, normalized for each cell to the average density of the first three time points. Bouton density in focally lesioned animals decreases within 24 hr (time: 24 hr $p < 0.05$; 48 hr $p < 0.05$; 72 hr $p < 0.01$; between groups $p < 0.01$), while it remains constant in control animals.

(D) Bouton survival fraction (between groups, $p < 0.01$). In (C) and (D), data from 27 axons in 9 animals are shown.

(E) Absolute bouton density in control and lesioned (72 hr after lesion) mice that were not previously imaged ($p < 0.01$; n = 16 axons, eight animals).

(F) Normalized bouton density in control mice and 72 hr after a focal retinal lesion. While excitatory bouton density does not change after lesioning ($p > 0.05$), inhibitory bouton density drops strongly ($p < 0.01$; n = 54 cells, 18 animals).

All error bars, SEM.

the measured axon from the border of the LPZ ($R = 0.6$; $p < 0.01$), with bouton density increasing steadily with distance from the border (Figure 5B).

One possibility is that the loss of inhibitory boutons reflects a response to reduced cortical activity rather than the ongoing functional reorganization known to occur after focal lesions (Keck et al., 2008). To determine if lowered cortical activity levels alone can lead to the observed changes in inhibitory cell boutons, we measured their dynamics following complete retinal lesions, as described above for inhibitory cell spines (Figures 3C–3E). We found that both bouton density (Figures 5C and 5D) and survival fraction (Figure 5E) decreased to the same degree as after focal retinal lesions. The changes occurred over a somewhat slower time scale, however, taking place over a 48 hr period compared with 24 hr in animals with focal lesions. These data suggest that the changes in bouton density are largely driven by a decrease in cortical activity.

Decreased Bouton Density Indicates Decreased Synapse Density

To determine whether the boutons were representative of actual inhibitory synapses, we performed immunostaining for pre- and postsynaptic markers of GABAergic synapses (Figure 6A). The vast majority of boutons both contained the vesicular GABA transporter (VGAT) and associated with gephyrin (84% ± 0.01%; $p < 0.05$ compared with controls where the image obtained through the GFP channel was rotated by 90° in order to assess the chance level for colocalization). Consistent with previous findings in hippocampal slice cultures (Wierenga et al., 2008), only 2% of GFP-positive boutons lacked both synaptic markers. These data show that most of the GFP-labeled axonal boutons indeed correspond to GABAergic synapses. To determine if there were fewer synapses after retinal lesions, we measured the density of boutons colocalizing with one or both of the synaptic markers in lesioned (72 hr after complete

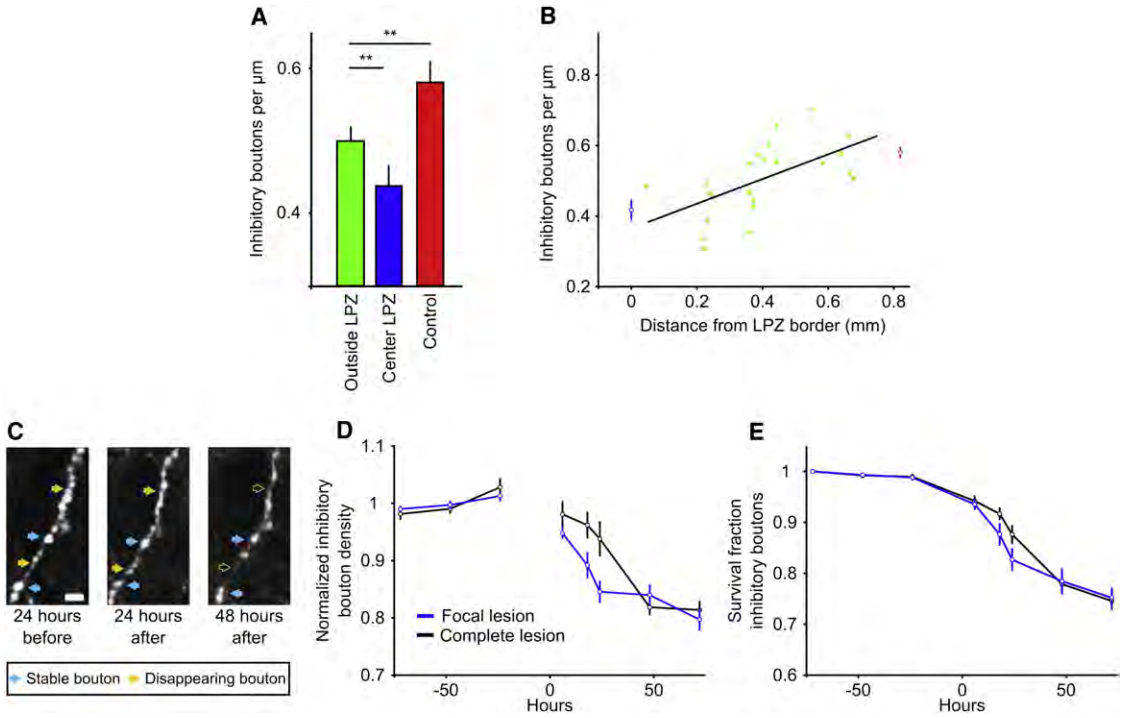

Figure 5. Inhibitory Axon Bouton Loss Is Not Limited to the LPZ

(A) Following a lesion (72 hr), inhibitory bouton density decreases outside the LPZ (green) relative to controls (red; $p < 0.01$), but is higher than bouton density in the center of the LPZ (blue; $p < 0.01$, n = 41 cells, 13 animals).

(B) Bouton density outside the LPZ is correlated ($R = 0.6$; $p = 0.003$) with distance from the border of the LPZ (at 0 mm). Green circles are individual cells. Average density is indicated for the center of the LPZ (blue) and control animals (red).

(C) Example z-projected images of the same axon before and after a complete retinal lesion. Arrows show disappearing (yellow) and stable (blue) boutons. Filled arrows indicate that the bouton is present, hollow arrows indicate that the bouton is absent. Scale bar, 5 µm.

(D) Normalized (average of first three time points) bouton density in completely lesioned animals (black) decreases within 48 hr (time: 48 hr, $p < 0.01$; 72 hr, $p < 0.01$) to the same degree observed in animals with focal lesions (blue; focal versus complete lesions, $p > 0.6$).

(E) Survival fraction of inhibitory boutons in animals with complete lesions decreased (48 hr, $p < 0.05$; 72 hr, $p < 0.05$) to the same degree as in animals with focal lesions (focal versus complete lesions, $p > 0.5$; in D and E, n = 30 cells, eight animals).

All error bars, SEM.

lesion) and control animals. We found that the fraction of GFP-labeled boutons with both synaptic markers did not change after lesioning (85% ± 0.02%), but that the overall GABAergic synapse density did decrease (Figure 6B), confirming the results observed with chronic structural imaging (Figures 4C and 4E).

Having established that inhibitory synapse density decreases following retinal lesions, we next determined if the bouton loss actually reflected a loss of functional GABAergic synapses in the cortical circuit. Layer 2/3 GABAergic cells are known to target both layer 2/3 pyramidal cell somata and the dendrites of layer 5 pyramidal cells located in layer 2/3 (Chen et al., 2011; Kätzel et al., 2011; Silberberg et al., 2005). As structural changes in excitatory pathways associated with functional circuit plasticity in adult visual cortex occur preferentially on layer 5, but not layer 2/3 cells (Hofer et al., 2009), we determined whether there was a reduction in functional inhibition onto layer 5 neurons. Therefore, we measured miniature inhibitory postsynaptic currents (mIPSCs) in layer 5 pyramidal cells in acute slices of visual cortex 48 hr after complete retinal lesions. We found that mIPSC frequency was decreased (Figures 6C and 6D), consistent with a reduction in the number of GABAergic synapses onto these cells. The amplitude of the mIPSCs was unchanged 48 hr after lesions, suggesting no postsynaptic receptor changes had occurred (Figures 6C and 6E). Together, these data indicate that following retinal lesions, there is a rapid decrease in the number of inhibitory synapses in the affected cortical region.

Finally, we compared the time course of changes in inhibitory neuron bouton and spine density after retinal lesions. Inside the LPZ in mice with focal lesions (Figure 7A), spine density (dashed line) was significantly decreased within 6 hr after the lesion, preceding the decrease in bouton density (solid line), which was significant only 24 hr after the lesion. The observation that changes of synaptic input structures (i.e., spines) of the interneurons precede changes in synaptic output structures (i.e., boutons) could possibly reflect a causal relation. In contrast, in animals with complete lesions (Figure 7B), spine and bouton density decrease over the same time course, 48 hr after the lesion. Together these data suggest that the exact timing of

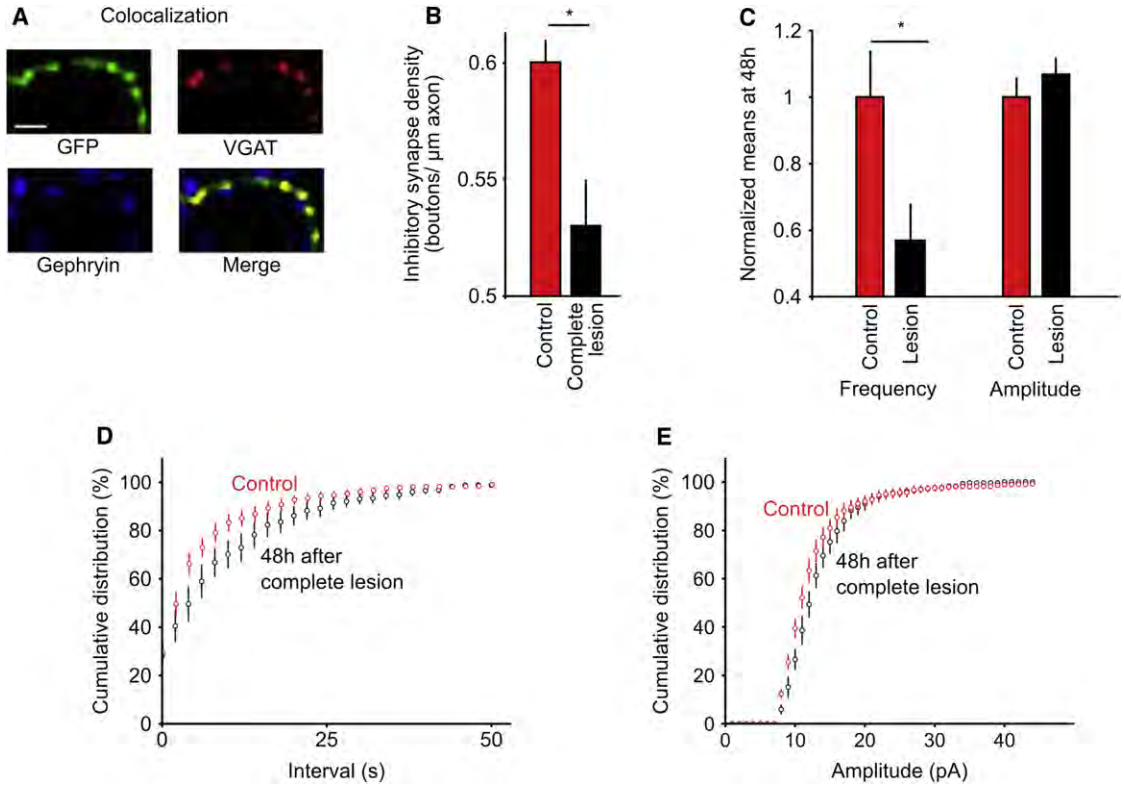

Figure 6. Inhibitory Bouton Loss Corresponds to Loss of Functional Inhibitory Synapses

(A) Example immunostainings (single z-plane) for GFP, gephyrin, and VGAT, and merged image. Scale bar, 5 µm.

(B) Inhibitory synapse density. Density of boutons with at least one GABAergic synaptic marker in control and lesion (72 hr after lesion) mice ($p < 0.05$; n = 130 axons, 20 animals).

(C) Mean frequency (left) and amplitude (right) of layer 5 neuron mIPSCs in controls (red) and 48 hr after a lesion (black; $p < 0.05$ for frequency, $p > 0.1$ for amplitude n = 33 cells, ten animals).

(D and E) Cumulative distribution function (CDF) of interval (D) or amplitude (E) of mIPSCs in control (red) and lesioned (black) animals (interval, $p < 0.01$).

All error bars, SEM.

these structural changes may depend on the nature of the input loss.

DISCUSSION

We have used chronic two-photon imaging to monitor structural plasticity of inhibitory neurons in adult mouse visual cortex. We observe that a subset of inhibitory neurons, many of which are NPY positive, carry dendritic spines. These spines, which likely form synapses with functional glutamatergic terminals, are dynamic over periods of a few days. Furthermore, we find that the axonal boutons of these interneurons also show a baseline level of turnover. Following removal of sensory input by focal retinal lesions, we observed a rapid loss of both dendritic spines and axonal boutons of inhibitory neurons. This effect is not spatially limited to the silenced cortical region, but gradually decreases with increasing distance from the border of the LPZ, and appears to be driven to a large degree, by reduced cortical activity levels. Because the changes in inhibitory structures precede increases in excitatory spine turnover (Keck et al., 2008), these data suggest that inhibitory structural plasticity may be the first step in cortical reorganization after sensory deprivation.

Inhibitory Neuron Spines

Most studies of synaptic structural plasticity in vivo thus far have focused on excitatory synapses, particularly postsynaptic dendritic spines. Here, we report that a subset of inhibitory neurons (mostly NPY positive cells) in adult mouse visual cortex bears dendritic spines. We have observed these spines under very different experimental conditions: in fixed tissue sections, in vivo and in acute cortical brain slices. Many, if not all, of these spines carry functional excitatory synapses, as revealed by immunohistochemistry and their response to glutamate uncaging. As has been observed for excitatory cells (Hofer et al., 2009; Holtmaat et al., 2006; Keck et al., 2008; Majewska et al., 2006; Trachtenberg et al., 2002; Zuo et al., 2005), inhibitory cell spines demonstrate a baseline level of turnover in naive adult animals over a period of days. Following sensory deprivation, changes to excitatory cell spines occur on the time scale of days (Hofer et al., 2009; Holtmaat et al., 2006; Keck et al., 2008; Trachtenberg et al., 2002; Zuo et al., 2005), typically in

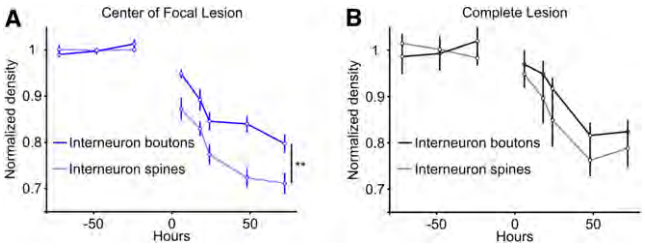

Figure 7. Temporal Relationship between Spine and Bouton Changes

(A) For cells in the center of the LPZ, spine (dashed line) density decreases to a larger degree than bouton (solid line) density (spines versus boutons $p < 0.01$; spines at 6 hr, $p < 0.05$; boutons at 24 hr, $p < 0.05$, n = 22 cells, four animals). (B) In animals with complete lesions, spine (dashed line) and bouton (solid line) density decline with the same time course (n = 19 cells, four animals). All error bars, SEM.

the form of increased dynamics, lasting for weeks to months. Here, we observe that spines on inhibitory neurons change much more rapidly—in the first 6 hr after deprivation—mainly via increased spine loss resulting in a decrease in spine density. This increase in dynamics occurs through the first 72 hr after deprivation, but not afterward, suggesting that inhibitory cell spine plasticity ends well before changes in excitatory spines subside.

Bouton Dynamics in Adult Cerebral Cortex

Axonal boutons in the naive cortex have been reported to demonstrate a baseline turnover in excitatory cells, the rate of which depends largely on cell type (De Paola et al., 2006; Stettler et al., 2006). Previous studies using chronic two-photon imaging of PV positive inhibitory neurons (Kuhlman and Huang, 2008), GABA positive inhibitory neurons (Chen et al., 2011) or GAD65 positive inhibitory neurons (Marik et al., 2010) demonstrated a baseline turnover of axonal boutons in adult cortex. Consistent with their results, we observed a turnover of axonal boutons of inhibitory neurons under control conditions in NPY, CCK, CR, and CB positive inhibitory neurons, suggesting that inhibitory synapses display a baseline level of plasticity in adult animals in most inhibitory cell types. Together these studies indicate that, similar to what has been observed for excitatory neurons (De Paola et al., 2006; Stettler et al., 2006), at least a fraction of inhibitory contacts consistently undergo turnover.

Furthermore, following retinal lesions, excitatory cell bouton density increases in the deprived region of the cortex within 6 hr and remains elevated for several weeks (Yamahachi et al., 2009). In complement, we see a decrease in inhibitory bouton density, although over a slightly slower time course—24 hr. These two results—increased numbers of excitatory boutons and decreased numbers of inhibitory boutons—could potentially work in conjunction to restore activity levels in the deprived region of the cortex.

The observed reduction in bouton density is consistent with data from previous studies showing reduced numbers of GAD puncta in the LPZ following retinal lesions in cats (Rosier et al., 1995) and a reduction in inhibitory bouton density following deprivation in somatosensory (Marik et al., 2010) and visual cortex (Chen et al., 2011), indicating that reduction of inhibitory structures after deprivation may be a general phenomenon and is potentially the first step in functional reorganization. Furthermore, the observed reduction of inhibitory bouton density likely corresponds to an actual loss of inhibitory synapses and not just to a change in GFP expression levels (either via reduction of GAD expression levels after plasticity or bleaching from two-photon imaging). Two points of evidence support this. First, mIPSC frequency (reflecting the number of inhibitory synapses) in excitatory layer 5 cells decreases 48 hr after a lesion, indicating a drop in the number of inhibitory inputs to these excitatory cells. Second, using immunohistochemistry, we see fewer boutons that colocalize with GABAergic pre- and postsynaptic markers following lesions, suggesting a decrease in the number of inhibitory synapses. Together, these data imply that following retinal lesions, inhibitory synapses in the visual cortex are lost.

Surprisingly, we do not observe recovery of the spine or bouton density, even several months after retinal lesions. This may be explained by the fact that we never observe a complete recovery of visual function in the LPZ. Even 6 months to 1 year following a lesion, the visually evoked activity levels in the LPZ are still lower than those outside the LPZ (Giannikopoulos and Eysel, 2006; Keck et al., 2008). Therefore, because the activity levels do not return to normal values, inhibitory drive may remain reduced to balance the reduced excitation levels. Consistent with this hypothesis, a previous study (Maffei and Turrigiano, 2008) suggests that removal of visual input by tetrodotoxin (TTX) injection into the eye causes a shift in the balance between excitation and inhibition onto layer 2/3 excitatory cells to favor excitation. Our data indicate that this shift toward excitation may occur partially by structural changes in inhibitory neurons.

A recent study in rat barrel cortex, combining viral labeling and chronic two-photon imaging to examine structural dynamics of GAD65 positive inhibitory neurons (Marik et al., 2010), suggests that following sensory deprivation via whisker plucking there is an increase in the growth and retraction of inhibitory neurons' axons in the deprived and, to a slightly lesser extent, the nondeprived barrels within 2 days of deprivation (Marik et al., 2010). We did not observe axonal remodeling in our study. This may indicate differences between barrel and visual cortical plasticity.

Mechanisms of Structural Changes

What leads to structural changes in inhibitory neurons? For the spines on inhibitory neurons, one plausible explanation is simply that the synapses undergo long-term depression (LTD), which has been demonstrated to occur after sensory deprivation in vivo (Rittenhouse et al., 1999). Reduction of spine density has been shown to be associated with LTD in excitatory cells (Nägerl et al., 2004), but has yet to be investigated in inhibitory neurons.

Mechanisms leading to the reduction of axonal boutons are less clear. Given that spine density decreases before bouton density, one possibility is that the effect is causal and a reduction of inputs to the inhibitory neuron, which presumably leads to a decrease in postsynaptic spiking, triggers a reduction of bouton density. As only a fraction of the boutons are eliminated,

however, it is unclear which boutons would be removed and which would be spared. Some insight may come from a previous study of inhibitory neurons in hippocampal cultures (Hartman et al., 2006): reduced activity of excitatory cells in the network caused a decrease in inhibitory synapses, but lowering activity levels of an individual inhibitory cell without altering activity in neighboring pyramidal neurons had no effect on inhibitory synapses. These results suggest that the activity of the postsynaptic excitatory cells may be responsible for changes to inhibitory boutons. Alternatively, signaling via second messengers, such as TNF-α released from astrocytes located at synapses (Fellin, 2009; Park and Bowers, 2010), could be involved as well.

Effect of Input Loss

In principle, the rapid changes of inhibitory structures following focal retinal lesions could reflect the onset of functional recovery in the visual cortex, or simply be caused by reduced cortical activity levels. To distinguish between these two possibilities, we compared the effects of focal and complete retinal lesions, the latter of which are not accompanied by functional recovery in the visual cortex (Keck et al., 2008). Therefore, any structural changes following this intervention can be considered a response to a decrease in cortical activity. For both spines and boutons of inhibitory cells, we observed a substantial decrease in density following both focal and complete retinal lesions. This result suggests that the loss of inhibitory structures may reflect a general reduction of inhibition after a decrease in cortical activity, which could be a result of either decreased activity levels in the inhibitory neurons themselves or in the activity levels of the network (as in Hartman et al., 2006).

The loss of spines and boutons following complete lesions, however, occurred over a somewhat slower time course than after focal lesions. One possible explanation for these differences in timing is that in the case of focal retinal lesions there is not only an overall drop in activity, but also competition between silenced and still active inputs stemming from cells located in regions of cortex adjacent to the LPZ. As competitive or Hebbian plasticity has been shown to develop in vitro over the time course of minutes to hours (Kirkwood and Bear, 1995), as opposed to homeostatic plasticity, which results from input loss and occurs over a period of days (Turrigiano and Nelson, 2004), it is conceivable that this competition causes a more rapid removal of silent inputs than the overall reduction of activity levels following complete retinal lesions.

Inhibitory Changes Outside the LPZ

We have previously demonstrated that structural changes in excitatory cells associated with functional recovery after a retinal lesion were restricted to the LPZ (Keck et al., 2008). In contrast, the structural changes of inhibitory neurons reported here occur in a gradient extending out from the border of the LPZ. How do inhibitory neurons outside the LPZ sense the reduction of activity in the LPZ? One possibility is that a reduction of input to layer 2/3 pyramidal cells located in the LPZ would lead to lower activity levels outside the LPZ by way of horizontal intracortical axon collaterals of these cells. Inhibitory neurons outside the LPZ would receive less excitatory input and react with a reduction of their spine and bouton density.

What could be the possible function of a reduction in inhibitory structures outside of the LPZ? We speculate that reduced inhibition potentially acts as a signal to excitatory layer 2/3 cells in these regions to increase axonal sprouting within the LPZ, known to occur following lesions to facilitate functional reorganization (Darian-Smith and Gilbert, 1994; Yamahachi et al., 2009). Consistent with this hypothesis, a recent study (Kreczko et al., 2009) demonstrated a decrease in GAD puncta on the somata of layer 2/3 excitatory cells following sensory deprivation, suggesting that a loss of inhibitory input to this specific group of cells does occur following input loss under at least some circumstances (but see Chen et al., 2011). Furthermore, Hu et al. (2009) measured expression levels of the immediate early genes zif268 and c-*fos*, which are commonly used as indicators for neuronal activity, to show that there is an increase in the activity levels of the cortex in cats directly adjacent to the LPZ in the days following a retinal lesion. These activity changes are consistent with a reduction of inhibition in the cortex surrounding the LPZ, and this change in activity level could trigger axonal dynamics on layer 2/3 pyramidal cells; however, further study is necessary to test this speculation.

Circuit Plasticity following Retinal Lesions

Data from intrinsic imaging and electrophysiology indicate that, following a focal retinal lesion, there is a reduction in the activity levels in the LPZ (Calford et al., 2003; Giannikopoulos and Eysel, 2006; Gilbert and Wiesel, 1992; Heinen and Skavenski, 1991; Kaas et al., 1990; Keck et al., 2008). Here, we demonstrate that soon after a focal retinal lesion, the density of inhibitory neuron spines carrying excitatory synapses decreases, presumably causing a loss of glutamatergic input to these cells. Loss of these excitatory inputs would lower these neurons' average spike rate, in turn, leading to a reduction of GABA release. Immediately following the spine loss, bouton density on these cells' axons decreases too. Together, these structural changes are likely to reduce the overall levels of inhibition in the LPZ and could potentially be part of a mechanism to restore the balance between excitation (which has been reduced by the retinal lesion) and inhibition in this region. We can only speculate whether similar processes occur on nonspiny inhibitory neurons, but it seems plausible that these cells would adjust their synaptic inputs and axonal outputs in a similar way.

We have previously shown that spine dynamics on layer 5 excitatory cells are increased 3-fold in the first month following focal lesions (Keck et al., 2008). This temporary increase in spine turnover likely reflects the rewiring of cortical circuits that underlies functional reorganization, since the functional and structural changes follow a similar time course and are correlated in magnitude. Previous work in fixed tissue in cat (Darian-Smith and Gilbert, 1994) and a more recent study using chronic two-photon imaging of virus labeled layer 2/3 pyramidal neurons in monkey (Yamahachi et al., 2009) suggest that the novel presynaptic inputs to layer 5 cell apical dendrites are derived from horizontal axons of layer 2/3 excitatory cells in regions adjacent to the LPZ. These axons start growing additional branches into the LPZ within hours after the lesion (Yamahachi et al., 2009). These structural changes likely contribute to the functional reorganization observed after a retinal lesion, as neurons in the LPZ begin

responding to stimuli located adjacent in visual space to the previous representation of the LPZ. The changes in inhibitory neurons observed here take place even before layer 5 spine turnover increases, suggesting that the reduced level of inhibition could be the first step in the cascade of plastic changes that eventually lead to structural plasticity of excitatory cells.

Based on these data, we propose the following temporal sequence for the functional reorganization after retinal lesions: within the first hours, physical removal of spines and boutons of inhibitory neurons leads to a reduction of inhibition, not only inside the LPZ, but also in neighboring cortex. This loss of inhibition facilitates competition-driven spine turnover on layer 5 pyramidal cells, presumably through the loss of inhibitory synapses on these cells (Figures 3C–3E). The reduced inhibition outside the LPZ and the resulting changes in activity levels may trigger layer 2/3 cells to extend their axons along the gradient of reduced inhibition leading into the LPZ. These axons would thus provide novel inputs that facilitate functional reorganization after a retinal lesion. Together these data suggest a critical role for inhibitory structural changes in the initiation of circuit reorganization.

EXPERIMENTAL PROCEDURES

All experimental procedures were carried out in compliance with the institutional guidelines of the Max Planck Society and the local government (Regierung von Oberbayern).

Retinal Lesions

The left retinae of ketamine/xylazine anaesthetized adult mice were focally photocoagulated with multiple confluent lesions (300 μm, 500–600 mW, 200 ms, corresponding to 10–15 degrees vertically and 20–40 degrees horizontally of visual angle) through a laser-adapted operating microscope, as described previously (Keck et al., 2008). In a separate group of mice, both retinae were photocoagulated in their entirety by multiple confluent laser lesions, 300 μm, 700–950 mW, 200 ms, directly aimed to and surrounding the optic disc in concentric circles to destroy all retinal ganglion cell fibers.

Intrinsic-Signal Imaging

Intrinsic imaging was used to determine the location of the LPZ following focal retinal lesions. Details of the imaging procedures and visual stimulation are described elsewhere (Mrsic-Flogel et al., 2005; Schuett et al., 2002). Briefly, the visual cortex was illuminated with 707 nm light and images (600 ms in duration) were captured with a cooled slow-scan CCD camera (ORA 2001, Optical Imaging, Rehovot, Israel), focused 200–300 μm below the cortical surface. During each 9 s stimulation trial, four blank frames were acquired, followed by visual stimulation, during which 11 frames were acquired. Visual stimuli consisted of square-shaped gratings (10–25°) presented at 24 positions on a screen located in the contralateral visual hemifield. Retinotopic maps were computed as previously described (Keck et al., 2008; Mrsic-Flogel et al., 2005; Schuett et al., 2002).

Two-Photon Imaging

We implanted cranial windows (Holtmaat et al., 2009) in ketamine/xylazine-anesthetized adult GAD65-GFP transgenic mice (age at surgery, 80–100 days), which express enhanced GFP under the GAD 65 promoter (López-Bendito et al., 2004). The skull overlying the right visual cortex was removed and replaced with a cover-glass window, leaving the dura intact. Animals recovered from surgery for at least 30 days before imaging started. We carried out two-photon imaging (Denk et al., 1990) using a custom-built microscope and a mode-locked Ti:sapphire laser (Mai Tai, Newport/Spectra Physics, Santa Clara, CA) at 912 nm through a 40× water immersion objective (0.8 NA, Olympus, Tokyo, Japan). Scanning and image acquisition were controlled by Fluoview software (Olympus); the average power delivered to the brain was <50 mW.

Imaging was carried out 72 hr before and after a retinal lesion (Figure 2A) at high resolution (1024 × 1024 pixels, 0.08 μm per pixel, 0.5 μm *z* step size). Imaging regions were repeatedly found by aligning the blood vessel pattern on the surface of the brain. Lower-resolution image stacks (512 × 512 pixels, 2.5 μm *z* step size) were acquired to visualize the dendritic and axonal branching pattern and the position of the soma, which, for the cells analyzed here, was confirmed to be located in cortical layer 1 or 2/3.

Cells in the LPZ were chosen such that they were located at least 50 μm from the borders to avoid any ambiguity. Cells located outside of the LPZ had cell bodies that were located >50 μm from the edge of the LPZ, as determined using intrinsic imaging within 3 days after the lesion. Distance from the border of the LPZ was calculated based on the position of the axon or, in the case of dendritic measurements, the cell body. High-resolution images were used for the analysis of dendritic spines and axonal boutons. Image analysis was carried out using ImageJ (US National Institutes of Health, Bethesda, MD) and performed in three dimensional *z* stacks. Analysis of spines and boutons were restricted to cortical layers 1 and 2/3 (0–200 μm below the cortical surface). All protrusions, spines and filopodia were counted, including those that extended in the z axis. Spines and boutons were counted without the knowledge of experimental condition. Survival fraction is calculated at each time point as the number of boutons or spines still present that were present at the first time point as a fraction of the total number of initial boutons or spines. In total, we analyzed 16,259 boutons and 9633 spines over 9–12 time points.

Immunohistochemistry

GAD65-GFP animals were deeply anaesthetized and cardially perfused first with saline (0.9% NaCl solution with 2.8 mg/liter heparin and 5 mg/liter lidocaine) and then with chilled 4% paraformaldehyde (4°C) for 30 min. Perfused brains were transferred to 30% sucrose solution for 2 days, after which they were sectioned coronally at 30 μm thickness. For analysis of excitatory and inhibitory synapses and inhibitory neuron cell type, the GFP signal in GABAergic neurons was amplified by immunofluorescence staining (chicken antibody to GFP, 1:1,000, Chemicon). GABAergic synapses were visualized by fluorescent labeling of VGAT (rabbit antibody to VGAT, 1:200, Synaptic Systems, Göttingen, Germany) and gephyrin (mouse antibody to gephyrin, 1:400, Synaptic Systems), as described previously (Wierenga et al., 2008). Glutmatergic synapses were visualized by fluorescent labeling of VGlut (rabbit α-VGlut1, 1:400, Synaptic Systems), as described previously (Becker et al., 2008). Cell type-specific markers were visualized by the fluorescence labeling of GABA (rabbit antibody to GABA, 1:2,000, Sigma), somatostatin (rat antibody to SOM, 1:500, Chemicon), Calretinin (rabbit antibody to CR, 1:1000, Swant), Neuropeptide Y (rabbit antibody to NPY, 1:1000, Immunostar), and Parvabulmin (mouse antibody to PV, 1:2000, Swant).

Immunofluorescence labeling was visualized with confocal imaging and analyzed in three-dimensional image stacks. Each channel was filtered and thresholded before determining the colocalization of GFP-labeled boutons or spines with pre- and postsynaptic markers for GABAergic synapses or with postsynaptic markers for glutamatergic synapses, or GFP-labeled somas with cell type-specific markers. Analysis was performed blind to experimental condition. Because of high background staining with the NPY antibody (Wierenga et al., 2010), cells were only considered positive when they were considerably brighter than their neighbors. Cell type analyses for these stainings were performed blindly multiple (2–3) times to ensure reliability. In total, we analyzed 1441 boutons from 130 cells in 20 mice and 469 spines from 30 cells in four mice. For cell type, we analyzed 752 cells in ten mice.

Miniature IPSC Recordings

Forty-eight hours after a complete retinal lesion or a sham-lesion (anesthesia, followed by atropine applied to the eye), deeply anaesthetized mice (p90-120) were perfused with 10 ml cold (4°C) artificial cerebral spine fluid (ACSF; in mM, 126 NaCl, 25 $NaHCO_3$, 25 Glucose × H_2O, 3.5 KCl, 1 NaH_2PO_4 × H_2O, 0.5 $MgSO_4$ × 7 H_2O and 1 $CaCl_2$ × 2 H_2O, osmolarity approximately 325 milliosmol/kg) saturated with 95% O_2/5% CO_2, after which the brain

was removed and coronally sliced (300 μm thick, Vibratome 3000, Leica, Wetzlar, Germany) to contain both hemispheres of primary visual cortex. Slices were incubated for 30 min in a holding chamber at 34°C and then 30 min at room temperature (24°C) before recording from layer 5 pyramidal neurons at room temperature.

Neurons were recorded using whole-cell patch clamp in voltage clamp mode on an upright microscope (Olympus, Tokyo, Japan) using differential interference contrast. Cell type was confirmed post-hoc in a subset of experiments using biocytin staining. Patch pipettes had a tip resistance of 3–5 MΩ and were filled with intracellular solution (in mM, 120 K-Gluconat, 10 KCl, 20 HEPES, 5 NaCl, and 12 Mg^{2+}-ATP [pH 7.20], osmolarity 292 milliosmol/kg).

Miniature inhibitory postsynaptic currents (mIPSCs) were recorded in an ACSF bath containing 1 μM Tetrodotoxin (TTX) and 250 μM Trichlormethiazide (TCM). Cells were voltage clamped at −70 mV (corrected for liquid junction potential) with an Axopatch 200B amplifier (Molecular Devices, Sunnyvale, CA), using custom software written in Labview (National Instruments, Austin, TX). Neurons that had a change in membrane potential or input resistance of greater than 10% during the recording time were excluded from the analysis. In a subset of experiments, 10 μM (±)-3-(2-carboxypiperazin-4-yl)propyl-1-phosphonic acid (CPP) to block N-methyl-d-aspartate (NMDA) receptors and 10 μM 2,3-dihydro-6-nitro-7-sulphamoyl-benzo(f) quinoxaline (NBQX) to block α-amino-3- hydroxy-5-methylisoxazole-4-propionic acid (AMPA) receptors were added to the bath, which had no effect on the distribution of frequency or amplitude of the mIPSCs. In a separate subset of experiments, 10 μM bicucculine was added to the bath, which eliminated all mIPSCs. mIPSC analysis was done with custom software written in Matlab (Mathworks, Natick, MA) and blind to the experimental condition. mIPSCs were detected based on amplitudes greater than 5 pA, and 20%–80% rise times of less than 1 ms. For each cell, 50 detected events were used. In total, we recorded from 33 cells in ten animals.

Two-Photon Glutamate Uncaging

Acute coronal slices (300 μm thick) of primary visual cortex were prepared in chilled dissection solution (in mM: 110 choline chloride, 25 $NaHCO_3$, 25 D-glucose, 11.6 Na-ascorbate, 7 $MgCl_2$, 3.1 Na-pyruvate. 2.5 KCl, 1.25 $NaH2PO_4$, 0.5 $CaCl_2$) from 37- to 44-day-old transgenic GAD65-GFP mice, as described above. Slices were incubated in ACSF (in mM: 127 $NaCl_2$, 25 $NaHCO_3$, 25 D-glucose, 2.5 KCl, 1 $MgCl_2$, 2 $CaCl_2$, 1.25 NaH_2PO_4) saturated with carbogen (95%O_2, 5%CO_2) at 35°C until use. In the recording chamber, the extracellular solution (at room temperature 24°C) consisted of ACSF, saturated with carbogen, and containing compounds to isolate AMPA type glutamate receptor currents, facilitate voltage-clamp and uncage glutamate (in mM: 0.01 CPP, 0.2 [+]-α-Methyl-4-carboxyphenylglycine [MCPG], 10 tetraethylammonium chloride [TEA-Cl], 2 4-AP, 0.5 4-ethylphenylamino-1,2-dimethyl-6-methylaminopyrimidinium chloride (ZD 7288), 0.001 TTX, 1 Trolox, 2.5 MNI-caged L-glutamate). Two-photon imaging was performed with a custom microscope (objective: 60×, 0.9 numerical aperture; Olympus). The light beams from two Ti:Sapphire lasers, one for imaging (Mai Tai) the other for glutamate uncaging (Millenia/Tsunami; Newport/Spectra Physics), were combined with a polarizing beam splitting cube and scanned by the same scanner (Yanus IV; Till Photonics, Gräfelfing, Germany). The intensity of each beam was independently controlled with electro-optical modulators (350–80 LA; Conoptics, Danbury, CT). Photomultipliers (Hamamatsu, Tokyo, Japan) recorded both epi- and transfluorescence. Image acquisition and two-photon uncaging was controlled by custom software written in Labview. Slices were screened for GFP positive spiny interneurons (at 930 nm). By simultaneously acquiring a laser Dodt-contrast image (Yasuda et al., 2004) of the slice anatomy, the search was limited to L2/3 of primary visual cortex. Somatic whole-cell patch recordings (pipette resistance, 3–4 MΩ; internal solution, in mM: 135 $CsMeSO_4$, 10 HEPES, 10 Na-phosphocreatine, 4 $MgCl_2$, 4 Na-ATP, and 0.4 Na-GTP, 5 EGTA, 0.1 spermine, 5 QX-314, 0.03 Alexa-594) were performed on identified GFP positive spiny interneurons. Data were acquired using a Multiclamp 700B patch amplifier, controlled with custom software (Molecular Devices, Sunnyvale, CA). For each spine analyzed, we recorded its direct response to glutamate uncaging next to its head and subsequently estimated the possible contribution from dendritic glutamate receptors by uncaging at the same distance from the dendrite at a neighboring location void of spines (see Figure 1F, lower left panel). For glutamate uncaging, the intensity of the 720 nm laser was set high (40–80 mW at the back aperture of the objective) for 0.4 ms when the beam passed the desired location during frame scanning.

Data analysis was performed with custom software written in Matlab. After baseline subtraction, five to ten traces from each stimulation position were averaged. For spine responses the amplitude and time of peak of the current were determined. The possible contribution from dendritic receptors was estimated as the dendritic current response at the time of the peak of the direct spine response (see Figure 1F). The distance between the uncaging location and the dendrite was determined with respect to the dendritic edge at the half maximal level of its transverse intensity profile.

Statistics

All plots show mean ± SEM. Comparisons were made using either Kolmogorov-Smirnov (K-S) test for cumulative distributions, a one or two-way ANOVA with Bonferroni post-hoc test, a t test, or a Mann-Whitney test (for non-normally distributed data). *$p < 0.05$, **$p < 0.01$.

ACKNOWLEDGMENTS

This work was supported by the Max Planck Society (T.K., V.S., R.I.J., C.J.W., T.B., and M.H.), the Amgen Foundation (R.I.J.), Marie Curie grants IEF #40528 and ERG #256284 (C.J.W.), the International Human Frontier Science Program Organization (V.S.), and the German Research Foundation (U.T.E.: SFB 874; M.H.: SFB 870). The research leading to these results has received funding from the European Community's Seventh Framework Programme [FP2007-2013] under grant agreement no 223326 (M.H.). The transgenic mice were kindly provided by Gábor Szabó (Budapest, Hungary). We would like to thank Valentin Stein and Alexander J. Krupp for assistance with electrophysiology data analysis, and Volker Staiger and Claudia Huber for technical assistance.

Accepted: June 20, 2011
Published: September 7, 2011

REFERENCES

Arellano, J.I., Benavides-Piccione, R., Defelipe, J., and Yuste, R. (2007). Ultrastructure of dendritic spines: correlation between synaptic and spine morphologies. Front Neurosci *1*, 131–143.

Azouz, R., Gray, C.M., Nowak, L.G., and McCormick, D.A. (1997). Physiological properties of inhibitory interneurons in cat striate cortex. Cereb. Cortex *7*, 534–545.

Becker, N., Wierenga, C.J., Fonseca, R., Bonhoeffer, T., and Nägerl, U.V. (2008). LTD induction causes morphological changes of presynaptic boutons and reduces their contacts with spines. Neuron *60*, 590–597.

Calford, M.B., Wright, L.L., Metha, A.B., and Taglianetti, V. (2003). Topographic plasticity in primary visual cortex is mediated by local corticocortical connections. J. Neurosci. *23*, 6434–6442.

Chen, J.L., Lin, W.C., Cha, J.W., So, P.T., Kubota, Y., and Nedivi, E. (2011). Structural basis for the role of inhibition in facilitating adult brain plasticity. Nat. Neurosci. *14*, 587–594.

Darian-Smith, C., and Gilbert, C.D. (1994). Axonal sprouting accompanies functional reorganization in adult cat striate cortex. Nature *368*, 737–740.

De Paola, V., Holtmaat, A., Knott, G., Song, S., Wilbrecht, L., Caroni, P., and Svoboda, K. (2006). Cell type-specific structural plasticity of axonal branches and boutons in the adult neocortex. Neuron *49*, 861–875.

Denk, W., Strickler, J.H., and Webb, W.W. (1990). Two-photon laser scanning fluorescence microscopy. Science *248*, 73–76.

Eysel, U.T. (1982). Functional reconnections without new axonal growth in a partially denervated visual relay nucleus. Nature *299*, 442–444.

Fellin, T. (2009). Communication between neurons and astrocytes: relevance to the modulation of synaptic and network activity. J. Neurochem. *108*, 533–544.

Feng, G., Mellor, R.H., Bernstein, M., Keller-Peck, C., Nguyen, Q.T., Wallace, M., Nerbonne, J.M., Lichtman, J.W., and Sanes, J.R. (2000). Imaging neuronal subsets in transgenic mice expressing multiple spectral variants of GFP. Neuron *28*, 41–51.

Freund, T.F., and Buzsáki, G. (1996). Interneurons of the hippocampus. Hippocampus *6*, 347–470.

Froemke, R.C., Merzenich, M.M., and Schreiner, C.E. (2007). A synaptic memory trace for cortical receptive field plasticity. Nature *450*, 425–429.

Giannikopoulos, D.V., and Eysel, U.T. (2006). Dynamics and specificity of cortical map reorganization after retinal lesions. Proc. Natl. Acad. Sci. USA *103*, 10805–10810.

Gilbert, C.D., and Wiesel, T.N. (1992). Receptive field dynamics in adult primary visual cortex. Nature *356*, 150–152.

Grutzendler, J., Kasthuri, N., and Gan, W.B. (2002). Long-term dendritic spine stability in the adult cortex. Nature *420*, 812–816.

Harris, K.M., and Stevens, J.K. (1989). Dendritic spines of CA 1 pyramidal cells in the rat hippocampus: serial electron microscopy with reference to their biophysical characteristics. J. Neurosci. *9*, 2982–2997.

Hartman, K.N., Pal, S.K., Burrone, J., and Murthy, V.N. (2006). Activity-dependent regulation of inhibitory synaptic transmission in hippocampal neurons. Nat. Neurosci. *9*, 642–649.

Heinen, S.J., and Skavenski, A.A. (1991). Recovery of visual responses in foveal V1 neurons following bilateral foveal lesions in adult monkey. Exp. Brain Res. *83*, 670–674.

Hendry, S.H., and Jones, E.G. (1988). Activity-dependent regulation of GABA expression in the visual cortex of adult monkeys. Neuron *1*, 701–712.

Hensch, T.K. (2005). Critical period mechanisms in developing visual cortex. Curr. Top. Dev. Biol. *69*, 215–237.

Hofer, S.B., Mrsic-Flogel, T.D., Bonhoeffer, T., and Hübener, M. (2009). Experience leaves a lasting structural trace in cortical circuits. Nature *457*, 313–317.

Holtmaat, A., Wilbrecht, L., Knott, G.W., Welker, E., and Svoboda, K. (2006). Experience-dependent and cell-type-specific spine growth in the neocortex. Nature *441*, 979–983.

Holtmaat, A., Bonhoeffer, T., Chow, D.K., Chuckowree, J., De Paola, V., Hofer, S.B., Hübener, M., Keck, T., Knott, G., Lee, W.C., et al. (2009). Long-term, high-resolution imaging in the mouse neocortex through a chronic cranial window. Nat. Protoc. *4*, 1128–1144.

Hu, T.T., Laeremans, A., Eysel, U.T., Cnops, L., and Arckens, L. (2009). Analysis of c-fos and zif268 expression reveals time-dependent changes in activity inside and outside the lesion projection zone in adult cat area 17 after retinal lesions. Cereb. Cortex *19*, 2982–2992.

Kaas, J.H., Krubitzer, L.A., Chino, Y.M., Langston, A.L., Polley, E.H., and Blair, N. (1990). Reorganization of retinotopic cortical maps in adult mammals after lesions of the retina. Science *248*, 229–231.

Kätzel, D., Zemelman, B.V., Buetfering, C., Wölfel, M., and Miesenböck, G. (2011). The columnar and laminar organization of inhibitory connections to neocortical excitatory cells. Nat. Neurosci. *14*, 100–107.

Kawaguchi, Y., Karube, F., and Kubota, Y. (2006). Dendritic branch typing and spine expression patterns in cortical nonpyramidal cells. Cereb. Cortex *16*, 696–711.

Keck, T., Mrsic-Flogel, T.D., Vaz Afonso, M., Eysel, U.T., Bonhoeffer, T., and Hübener, M. (2008). Massive restructuring of neuronal circuits during functional reorganization of adult visual cortex. Nat. Neurosci. *11*, 1162–1167.

Kirkwood, A., and Bear, M.F. (1995). Elementary forms of synaptic plasticity in the visual cortex. Biol. Res. *28*, 73–80.

Knott, G.W., Holtmaat, A., Wilbrecht, L., Welker, E., and Svoboda, K. (2006). Spine growth precedes synapse formation in the adult neocortex in vivo. Nat. Neurosci. *9*, 1117–1124.

Komiyama, T., Sato, T.R., O'Connor, D.H., Zhang, Y.X., Huber, D., Hooks, B.M., Gabitto, M., and Svoboda, K. (2010). Learning-related fine-scale specificity imaged in motor cortex circuits of behaving mice. Nature *464*, 1182–1186.

Kreczko, A., Goel, A., Song, L., and Lee, H.K. (2009). Visual deprivation decreases somatic GAD65 puncta number on layer 2/3 pyramidal neurons in mouse visual cortex. Neural Plast. *2009*, 415135.

Kuhlman, S.J., and Huang, Z.J. (2008). High-resolution labeling and functional manipulation of specific neuron types in mouse brain by Cre-activated viral gene expression. PLoS One *3*, e2005.

Lee, W.C., Huang, H., Feng, G., Sanes, J.R., Brown, E.N., So, P.T., and Nedivi, E. (2006). Dynamic remodeling of dendritic arbors in GABAergic interneurons of adult visual cortex. PLoS Biol. *4*, e29.

Lee, W.C., Chen, J.L., Huang, H., Leslie, J.H., Amitai, Y., So, P.T., and Nedivi, E. (2008). A dynamic zone defines interneuron remodeling in the adult neocortex. Proc. Natl. Acad. Sci. USA *105*, 19968–19973.

López-Bendito, G., Sturgess, K., Erdélyi, F., Szabó, G., Molnár, Z., and Paulsen, O. (2004). Preferential origin and layer destination of GAD65-GFP cortical interneurons. Cereb. Cortex *14*, 1122–1133.

Maffei, A., and Turrigiano, G.G. (2008). Multiple modes of network homeostasis in visual cortical layer 2/3. J. Neurosci. *28*, 4377–4384.

Majewska, A.K., Newton, J.R., and Sur, M. (2006). Remodeling of synaptic structure in sensory cortical areas in vivo. J. Neurosci. *26*, 3021–3029.

Marik, S.A., Yamahachi, H., McManus, J.N., Szabo, G., and Gilbert, C.D. (2010). Axonal dynamics of excitatory and inhibitory neurons in somatosensory cortex. PLoS Biol. *8*, e1000395.

Martínez, A., Ruiz, M., and Soriano, E. (1999). Spiny calretinin-immunoreactive neurons in the hilus and CA3 region of the rat hippocampus: local axon circuits, synaptic connections, and glutamic acid decarboxylase 65/67 mRNA expression. J. Comp. Neurol. *404*, 438–448.

Mrsic-Flogel, T.D., Hofer, S.B., Creutzfeldt, C., Cloëz-Tayarani, I., Changeux, J.P., Bonhoeffer, T., and Hübener, M. (2005). Altered map of visual space in the superior colliculus of mice lacking early retinal waves. J. Neurosci. *25*, 6921–6928.

Nägerl, U.V., Eberhorn, N., Cambridge, S.B., and Bonhoeffer, T. (2004). Bidirectional activity-dependent morphological plasticity in hippocampal neurons. Neuron *44*, 759–767.

Nägerl, U.V., Köstinger, G., Anderson, J.C., Martin, K.A., and Bonhoeffer, T. (2007). Protracted synaptogenesis after activity-dependent spinogenesis in hippocampal neurons. J. Neurosci. *27*, 8149–8156.

Park, K.M., and Bowers, W.J. (2010). Tumor necrosis factor-alpha mediated signaling in neuronal homeostasis and dysfunction. Cell. Signal. *22*, 977–983.

Peters, A., and Regidor, J. (1981). A reassessment of the forms of nonpyramidal neurons in area 17 of cat visual cortex. J. Comp. Neurol. *203*, 685–716.

Rittenhouse, C.D., Shouval, H.Z., Paradiso, M.A., and Bear, M.F. (1999). Monocular deprivation induces homosynaptic long-term depression in visual cortex. Nature *397*, 347–350.

Rosier, A.M., Arckens, L., Demeulemeester, H., Orban, G.A., Eysel, U.T., Wu, Y.J., and Vandesande, F. (1995). Effect of sensory deafferentation on immunoreactivity of GABAergic cells and on GABA receptors in the adult cat visual cortex. J. Comp. Neurol. *359*, 476–489.

Schuett, S., Bonhoeffer, T., and Hübener, M. (2002). Mapping retinotopic structure in mouse visual cortex with optical imaging. J. Neurosci. *22*, 6549–6559.

Silberberg, G., Grillner, S., LeBeau, F.E., Maex, R., and Markram, H. (2005). Synaptic pathways in neural microcircuits. Trends Neurosci. *28*, 541–551.

Stettler, D.D., Yamahachi, H., Li, W., Denk, W., and Gilbert, C.D. (2006). Axons and synaptic boutons are highly dynamic in adult visual cortex. Neuron *49*, 877–887.

Trachtenberg, J.T., Chen, B.E., Knott, G.W., Feng, G., Sanes, J.R., Welker, E., and Svoboda, K. (2002). Long-term in vivo imaging of experience-dependent synaptic plasticity in adult cortex. Nature *420*, 788–794.

Turrigiano, G.G., and Nelson, S.B. (2004). Homeostatic plasticity in the developing nervous system. Nat. Rev. Neurosci. *5*, 97–107.

Wierenga, C.J., Becker, N., and Bonhoeffer, T. (2008). GABAergic synapses are formed without the involvement of dendritic protrusions. Nat. Neurosci. *11*, 1044–1052.

Wierenga, C.J., Müllner, F.E., Rinke, I., Keck, T., Stein, V., and Bonhoeffer, T. (2010). Molecular and electrophysiological characterization of GFP-expressing CA1 interneurons in GAD65-GFP mice. PLoS ONE *5*, e15915.

Xu, T., Yu, X., Perlik, A.J., Tobin, W.F., Zweig, J.A., Tennant, K., Jones, T., and Zuo, Y. (2009). Rapid formation and selective stabilization of synapses for enduring motor memories. Nature *462*, 915–919.

Yamahachi, H., Marik, S.A., McManus, J.N., Denk, W., and Gilbert, C.D. (2009). Rapid axonal sprouting and pruning accompany functional reorganization in primary visual cortex. Neuron *64*, 719–729.

Yang, G., Pan, F., and Gan, W.B. (2009). Stably maintained dendritic spines are associated with lifelong memories. Nature *462*, 920–924.

Yasuda, R., Nimchinsky, E.A., Scheuss, V., Pologruto, T.A., Oertner, T.G., Sabatini, B.L., and Svoboda, K. (2004). Imaging calcium concentration dynamics in small neuronal compartments. Sci. STKE *2004*, pl5.

Zuo, Y., Yang, G., Kwon, E., and Gan, W.B. (2005). Long-term sensory deprivation prevents dendritic spine loss in primary somatosensory cortex. Nature *436*, 261–265.